Torsional Relaxation and Friction on the Nanometer Length Scale: Comparison of Small-Molecule Rotation in Poly(dimethylsiloxane) and Poly(isobutylene)

Mark M. Somoza, Mikhail I. Sluch, and Mark A. Berg*

Department of Chemistry and Biochemistry, University of South Carolina, Columbia, South Carolina 29208

Received July 23, 2002; Revised Manuscript Received February 4, 2003

ABSTRACT: The rotation time of dissolved anthracene is used as a measure of the viscosity on a nanometer-sized object, and this "nanoviscosity" is compared to the ordinary macroscopic viscosity of polymers. Measurements in poly(dimethylsiloxane) (PDMS) as a function of the chain length extend from a small oligomer (M = 162 g/mol) to the entangled polymer (M = 139 000 g/mol). The results are compared to similar ones in poly(isobutylene) (PIB) [*J. Phys. Chem. B* **2002,** *106,* 7385]. Despite many similarities in the static structures of PDMS and PIB, qualitative differences are found in the behavior of the nanoviscosity. The nanoviscosity in the infinite polymer limit is 15 000 times lower in PDMS than in PIB. The difference arises in the oligomeric region, where the nano- and macroviscosities diverge at a much shorter chain length in PDMS than in PIB. Because the barriers between torsional conformations are much lower in PDMS than in PIB, these findings are consistent with the hypothesis that the divergence of macro- and nanoviscosities is dependent on a dynamic correlation length involving torsional relaxation. This divergence represents a change from the Stokes−Einstein−Debye behavior characteristic of small-molecule solvents to the Rouse behavior characteristic of polymers. Literature data on *n*-alkanes are reexamined in this context. The alkanes are an intermediate case between PDMS and PIB, both in terms of torsional barrier height and in terms of the chain length where macro- and nanoviscosities diverge.

I. Introduction

Even for an object of micron size, simple hydrodynamics provides an excellent description of the object's motion in a polymer fluid. However, as the object becomes smaller than various characteristic lengths of the polymer chain, deviations from simple hydrodynamic motion are expected. For example, the Stokes−Einstein−Debye (SED) model,[1,2] which applies the macroscopic viscosity to predictions of small-solute diffusion and rotation, works well in small-molecule fluids. However, in long chain polymer melts and rubbers, small molecules diffuse many orders of magnitude faster than predicted by the SED model.[3,4] In other words, the viscosity experienced by a large object, i.e., the macroviscosity, is different from the viscosity experienced by a small object. This point of view is firmly established in models such as the Rouse model,[5,6] which assumes that the macroviscosity is different from the "segmental friction". Although their existence is widely accepted, size-dependent dynamics in polymers are still poorly characterized by direct experiments, and the basic mechanisms governing them are not well established. This paper presents measurements of anthracene rotation in poly(dimethylsiloxane) (PDMS) that are compared to similar results that we recently reported in poly(isobutylene) (PIB).[7] The comparison supports our previous interpretation that the rate of torsional barrier crossing is the controlling factor in the hydrodynamic interactions between the polymer and nanometer-scale particles.

In a previous paper, we showed that the rotation time of anthracene measures the friction on a nanometer-sized object, i.e., the nanoviscosity.[7] Rather than varying the object size with a fixed polymer length, we looked at size effects by keeping the object size fixed and varying the length of the polymer chain. In small-molecule fluids, the nano- and macroviscosities are equal, in accord with the SED model. In PIB, the nano- and macroviscosities are equal for small oligomers but diverge sharply once the chain length exceeds ℓ_{SED} = 17, where ℓ is the number of backbone bonds.[8] This length does not correspond to any standard static length scale of the polymer. For example, it is longer than the characteristic ratio, C_∞ = 6.7, and shorter than the critical entanglement length, ℓ_e = 607.

We proposed that the important length is defined by a dynamic correlation length rather than a static one. This length is determined by the average distance between a point force on the polymer chain and the first torsional relaxation that can relieve the resulting stress within a given time. In PIB, the torsional barriers are high, and the relaxation probability for an individual bond is low during the rotation time of anthracene. However, if the chain is longer than ℓ_{SED}, there is a good probability for a torsional barrier crossing somewhere along the chain within the rotation time. If such a barrier crossing is probable, a relaxation channel is open that can accommodate the motion of a small object, but not the motion of a large object. As a result, the nano- and macroviscosities become different.

A comparison between PIB and PDMS is a good test of this proposal. Replacing the carbon−carbon backbone of PIB with a silicon−oxygen backbone generates PDMS (Figure 1). The size and shape of the repeat units of the two polymers are similar. In both polymers, gauche and trans torsional conformations have similar probabilities.[9,10] Although the Si−O−Si bond angle is larger than the corresponding angle in PIB,[9] measures of the chain's overall structure, such as the characteristic ratio,[11] the

* Corresponding author: e-mail berg@mail.chem.sc.edu; phone 803-777-1514; FAX 803-777-1456.

10.1021/ma021181n CCC: $25.00
Published on Web 03/26/2003

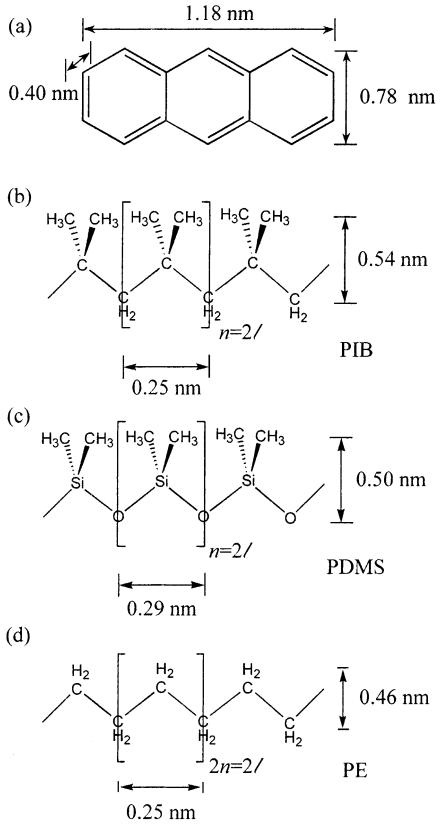

Figure 1. Structures, lengths, and van der Waals widths of the solute and polymers considered here: (a) anthracene, (b) poly(isobutylene), (c) poly(dimethylsiloxane), (d) *n*-alkanes.

entanglement length,[12] and self−diffusion coefficient,[13] are nearly identical in the two polymers.

Despite the strong similarity between the PIB's and PDMS's static structures, the kinetics of torsional relaxation are very different. In PIB, steric interaction between the methyl groups makes the barrier between gauche and trans conformations high compared to thermal energies at room temperature.[14] As a result, conformational changes occur relatively slowly, in the range of tens of nanoseconds. In PDMS, the longer backbone bonds and more open Si−O−Si bond angle removes the interaction of the methyl groups. Torsional transitions in PDMS are nearly barrierless compared to typical thermal energies[15,16] and should occur much more rapidly than in PIB.

If our proposal that the probability of torsional relaxation governs the divergence of the nano- and macroviscosities is correct, the divergence should occur for much shorter PDMS chains than for PIB chains. This paper presents measurements that test this prediction. The rotation rate of anthracene is measured in PDMS samples with chain lengths in the range l = 4−3760 (M = 162−139 000 g/mol). These rates are converted to nanoviscosities that can be compared to the ordinary macroviscosity. The behavior of PDMS with chain length is compared to that of PIB and found to differ significantly. These differences can be explained as arising from the difference in torsional relaxation rates. At the end of the paper, we reanalyze literature data on *n*-alkanes by similar methods. Relative to PIB and PDMS, *n*-alkanes have an intermediate torsional barrier height and have a divergence of nano- and macroviscosity at an intermediate chain length. A preliminary report of this work has appeared previously.[17]

This paper is not the first to consider small molecule motion, either diffusion or rotation, as a measure of a "local friction" in either pure polymers or in polymer solutions. This literature is too large to review completely here but can be found in refs 7 and 18−23 and references therein. The important features of this study relative to previous work are the use of a calibrated probe that gives absolute values of the nanoviscosity, the measurement of a range of chain lengths that spans the small-molecule to polymer regimes, and the comparison of two polymers closely related in structure, but different in torsional dynamics.

Two groups have looked at solute rotation in PDMS previously. Stein et al. measured the nanoviscosity with a polar solute for several chain lengths.[24] Subsequently, the same group used a nonpolar solute to measure the temperature dependence of the nanoviscosity.[25] Niemeyer and Bright measured rotation times in PDMS as a function of chain length, although they did not calibrate them to absolute nanoviscosities.[26]

Recently, a series of neutron and light scattering studies has been done on pure PDMS and PIB.[13,27−30] Differences are seen at short length scales. PDMS appears to be an ideal Rouse polymer, in the sense that intrachain friction is entirely absent at all measured length scales. For PIB, Rouse modeling of chain dynamics fails at short chain lengths. These differences are accounted for by adding an "internal viscosity" to the chain. Internal viscosity is usually attributed to torsional relaxation of the chain.[31,32]

We note that all of our experiments are done for a solute that is small relative to the polymer chain length but longer than the chain width (Figure 1). Because the solute is larger than the chain width, significant displacement of the chains is needed for solute motion, and good coupling of the solute and polymer is expected. It is also very difficult to accumulate voids of the same size as the solute. Both these features may change for very small solutes (e.g., He, O_2, CO_2) that may be able to move in cavities within the polymer matrix and whose rotation may not be as strongly coupled to adjacent polymer segments. The motion of these very small solutes may be governed by an "angstrom viscosity" that is determined by a different set of polymer characteristics and solvent−solute interactions than the nanoviscosity measured here. It is also plausible that there are other length scales between the nanometer scale and the macroscopic limit that define other mesoviscosities for other object sizes. We use the term "nanoviscosity" to specifically refer to the near one nanometer length scale probe in these experiments.

II. Summary of Previous Results

Anthracene as a Nanoviscometer. Before measurements of a molecular rotation time can be converted to nanoviscosities, the "nanoviscometer" must be calibrated and validated on known materials. Our previous paper discusses these issues in detail.[7] We summarize the results here.

Under appropriate circumstances, the molecular rotation time τ_r is governed by the same hydrodynamics that governs the motion of macroscopic objects:

$$\tau_r = \frac{\lambda V_h}{6kT}\eta + \tau_0 \qquad (1)$$

This modified Stokes−Einstein−Debye (SED) model[1,2]

of molecular rotation holds when the solvent molecules are smaller than the solute molecule.[33,34] In other words, in small-molecule solvents, the macro- and nanoviscosities are the same.

A number of factors are known to cause a failure of the SED model for some solutes, either in general or in specific classes of solvents. These include electrostatic solvent−solute interaction causing dielectric friction, solvent attachment by hydrogen-bonding, and flexible or irregularly shaped solutes. Anthracene has none of these problems.[35,36] In addition, the symmetry of anthracene, in combination with an accidental degeneracy in the diffusion constants for rotation around two of its axes, leads to single-exponential anisotropy decays rather than the multiexponential decays expected in the general case.[7] Thus, anthracene is a particularly good choice as a nanometer-sized viscometer.

We have measured anthracene's rotation time in a number of small-molecule solvents, including ones that are nonpolar, polar, and hydrogen-bonding.[7] Across all solvent classes and over a broad range of macroviscosity (0.3−60 cP), the times fit eq 1 to within a few picoseconds. The fit parameters, $\lambda V_h/6kT = 8.68$ ps/cP and $\tau_0 = 3.95$ ps, agree with the predictions for an ellipsoid of dimensions $1.18 \times 0.75 \times 0.42$ nm with slip boundary. These hydrodynamic dimensions are very close to anthracene's van der Waals dimensions of $1.18 \times 0.78 \times 0.40$ nm.

In more complex fluids, and in particular in polymers, the friction experienced by a nanometer-sized object may not be the same as the friction experienced by a macroscopic object. In these system, we invert eq 1 to define the nanoviscosity

$$\eta_{nm} = \frac{6kT}{\lambda V_h}(\tau_r - \tau_0) \tag{2}$$

in terms of the rotation time. The other parameters are taken from the small-molecule calibration experiments.

This definition of a nanoviscosity is very similar to standard procedures used to measure macroviscosity. In general, a viscometer is made by solving the hydrodynamic problem for a specific geometry appropriate to the apparatus. This solution gives the rate of an observable process, e.g., the rate of flow through a tube, in terms of the viscosity. Known samples are used to verify the hydrodynamic model and to calibrate the apparatus. The hydrodynamic problem is then inverted to obtain viscosities of unknowns from the observed rates. The same procedure has been followed in deriving eq 2, except that a nanometer-sized object has been used to make the measurement.

Results in PIB. In our previous paper,[7] we looked at the change in behavior between small-molecule solvents and polymeric solvents by measuring anthracene anisotropy decays in PIBs of various lengths. To facilitate comparison between different polymers, we characterized the length in terms of the number of backbone bonds

$$\ell = \sigma \frac{M}{M_r} \tag{3}$$

where M is the molecular weight, M_r is the molecular weight of the repeat unit ($M_r = 56$ g/mol for PIB), and σ is the number of backbone bonds per repeat unit ($\sigma = 2$ for PIB). Complications due to end effects and different averages of molecular weight are not large enough to affect our results and are ignored here.

Exponential−Nonexponential Transition. In small-molecule solvents, anthracene's anisotropy decays are always exponential, leading to a simple definition of the rotation time τ_r

$$r(t) = r_0 e^{-t/\tau_r} \tag{4}$$

In PIB, the decay shape changes abruptly from exponential to stretched exponential at a relatively short chain length ($\ell \approx 8$).

The stretched exponential anisotropy decay is described by

$$r(t) = r_0 \exp[-(t/\tau)^{\beta}] \tag{5}$$

The parameter β is a measure of the degree of nonexponentiality. The limit $\beta = 1$ corresponds to an exponential decay (eq 4) and decreasing values of β corresponding to increasing nonexponentiality. Stretched exponentials are often observed for various relaxation processes in viscous fluids.[37] The question of whether stretched relaxation is intrinsic or due to heterogeneity in the samples remains controversial.

Once this transition from exponential to stretched exponential has occurred, the shape of the decay does not change further. The value of β remains constant, even as the polymer increases in size from $\ell = 12$ to 3036 ($M = 350$ to 85 000 g/mol). We previously suggested that the transition to nonexponentiality is due to the development of conformational heterogeneity. This suggestion will be discussed further in section V and shown to be consistent with the PDMS results.

To determine a characteristic rotation time from these nonexponential decays, we use the fitting parameters τ and β from eq 5 to calculate an integral average rotation time

$$\tau_r = \int_0^\infty \frac{r(t)}{r_0}\,dt = \frac{\tau}{\beta}\Gamma(1/\beta) \tag{6}$$

where $\Gamma(x)$ is the gamma function and the second equality applies specifically to the stretched exponential function.[38] This function corresponds to the area under the decay curve, and as a result, its value is independent of the specific model function used to fit the decay curves. The integral average rotation time also reduces to the standard single-exponential decay time when $\beta = 1$.

The integral average rotation times τ_r are used in eq 2 to calculate the nanoviscosity. Although other characteristic times could be used, this procedure proved to be satisfactory for interpreting the results.

Low Value of r_0. The value of the initial anisotropy of anthracene in PIB, $r_0 = 0.27$, is distinctly lower than the maximum possible value of 0.4 or than the value found experimentally in small-molecule solvents ($r_0 = 0.34$).[36,40] It is possible that a partial reorientation is faster than our time resolution. Nonetheless, our results in short polymers agree with the SED model (eq 1), if the such hypothetical fast relaxations are ignored. This result shows that the observed slow reorientation is the correct one to use in measuring the nanoviscosity.

Divergence of Nano- and Macroviscosities. The nanoviscosity measured in PIB was compared to the kinematic viscosity on macroscopic objects η_∞ as a function

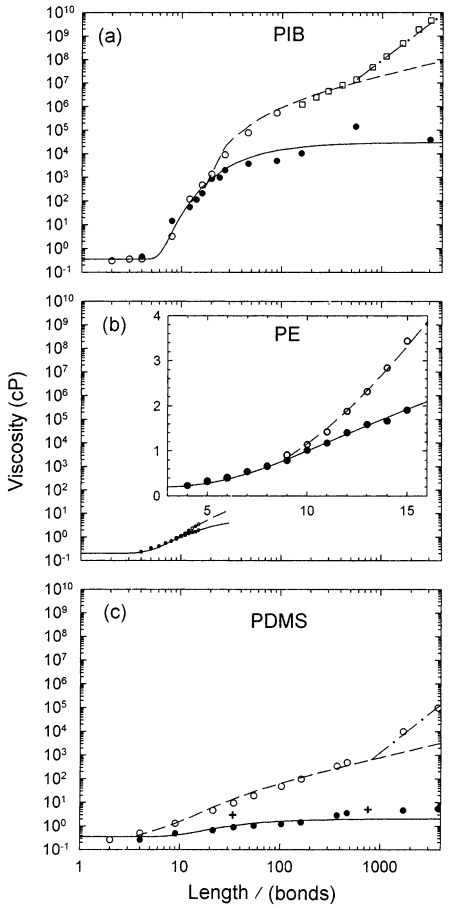

Figure 2. Macroviscosity (open symbols) and nanoviscosity (solid symbols) of (a) PIB, (b) *n*-alkanes [poly(ethylene) = PE], and (c) PDMS as a function of the number of backbone bonds ℓ. The data for PIB are from ref 7, and the *n*-alkane results are derived from the data of Luther and Benzler.[39] PDMS nanoviscosity measurements by Stein et al. are also shown (+).[24] The nanoviscosities are fit (solid curves) to eq 7 and the macroviscosities (dashed curves) to eq 8. Above the entanglement length, the macroviscosity is fit with a slope of 3.4 (dot−dashed lines). The length where the nanoviscosity diverges from the macroviscosity follows the trend in torsional barrier heights (PIB > *n*-alkanes > PDMS; Table 3). The inset to (b) uses expanded, linear scales.

of PIB chain length. The results are summarized in Figure 2a. Above $\ell = 5$, the PIB molecular shape becomes chainlike rather than compact, and the macroviscosity increases rapidly with chain length. The nanoviscosity remains the same as the macroviscosity until a longer length is reached at $\ell_{SED} = 17$. Above this length the macroviscosity continues to increase, until the entanglement length $\ell_e = 607$, where the increase becomes very steep. Above the divergence point at $\ell_{SED} = 17$, the nanoviscosity increases slightly before reaching an asymptotic value. Crossing the critical entanglement length has no effect on the nanoviscosity. For the longest PIB chains measured in our experiments, $\ell = 3036$ ($M = 85\,000$ g/mol), the nano- and macroviscosities differ by more than 5 orders of magnitude.

Although the overall behavior of the macro- and nanoviscosities is complex, a number of features can be rationalized. The approach of the nanoviscosity to its asymptotic value is described by the empirical formula

$$\eta_{nm}(\ell) = \eta_{nm}^{0} + (\eta_{nm}^{\infty} - \eta_{nm}^{0})e^{-A/\ell} \qquad (7)$$

Because the density of end group goes as $1/\ell$, the dependence on $1/\ell$ in eq 7 suggests that the slow approach to the asymptotic value is related to the loss of end effects. Fitting the PIB data with eq 7 leads to best fit values of $\eta_{nm}^{0} = 0.35$ cP, $\eta_{nm}^{\infty} = 3.0 \times 10^4$ cP, and $A = 70$. (Subscripts refer to solute size, and superscripts refer to polymer length.)

Once the behavior of the nanoviscosity is known, the increase of the macroviscosity above $\ell_{SED} = 17$ can be understood from a Rouse-like model. In the Rouse model, the macroviscosity is proportional to the chain length and to the "segmental viscosity."[5,6] We assume that the nanoviscosity is proportional to the segmental viscosity, and then we form a simple formula

$$\frac{\eta_{\infty}(\ell)}{\eta_{nm}(\ell)} = 1 + \begin{cases} B(\ell - \ell_{SED}) & \ell > \ell_{SED} \\ 0 & \ell < \ell_{SED} \end{cases} \qquad (8)$$

that interpolates between SED behavior

$$\eta_{\infty}(\ell) = \eta_{nm}(\ell) \qquad (9)$$

for small chains with $\ell < \ell_{SED}$, and Rouse behavior

$$\eta_{\infty}(\ell) \propto \ell\eta_{nm}(\ell) \qquad (10)$$

for chains with $\ell \gg \ell_{SED}$. As Figure 2a shows, this simple model accounts for the rise in the macroviscosity below the entanglement length and provides a specific way to parametrize the length dividing the SED and Rouse regimes. The fit curve for PIB macroviscosity in Figure 2a yields $\ell_{SED} = 17$ and $B = 0.75$.

The most important feature of Figure 2a and the one most difficult to rationalize is the divergence of macro- and nanoviscosities at $\ell_{SED} = 17$. This length is significantly longer than the obvious measures of static structure in the system (Table 1): the length where the PIB becomes chainlike (length ≫ width), the length where PIB becomes larger than anthracene (1.18 × 0.78 × 0.40 nm), or the length of where PIB develops multiple "segments" (C_{∞}).

We suggested that the important length scale is not a static one, but a dynamic one determined by the rate of torsional barrier crossings. This length is defined as the chain length needed for a torsional barrier crossing to become likely somewhere on the chain *during the rotation time*. The resulting change in chain conformation provides a channel for relaxation that is effective in accommodating the motion of a nanometer-sized object, but not in accommodating the motion of a large object.

III. Experimental Methods

The methyl-terminated PDMS samples were obtained from Gelest, were optically clear, and had typical polydispersities (M_w/M_n) of 1.8−2.0. Macroviscosity values for all of the samples were obtained from the manufacturer and are displayed in Table 2. The wide range of polymer viscosities and anthracene rotational rates required the use of several different methods of measuring rotation rates in different molecular weight ranges.

For all but the four highest molecular weight samples, the speed of the rotation required the use of transient dichroism to measure the rotation rates. In transient dichroism experiments,[43] an intense linearly polarized pump pulse selectively excites those anthracene molecules whose transition dipoles are aligned with the pulse's electric field. Because of the selective bleaching of the ground state and population of the excited state, the sample becomes dichroic; i.e., the transmission of light polarized parallel to the pump pulse is higher than

Table 1. Important Lengths in PIB, PDMS, and *n*-Alkanes Converted between Different Units

	PDMS[a]			PIB[b]			*n*-alkanes (PE)[c]		
	M (g/mol)	ℓ(bonds)	ℓ^d (nm)	M (g/mol)	ℓ(bonds)	ℓ^d (nm)	M (g/mol)	ℓ(bonds)	ℓ^d (nm)
chain width	127	3.4	0.50	120	4.3	0.54	50	3.5	0.46
C_∞[e]	233	6.3	0.92	190	6.8	0.86	102	7.3	0.92
exp−nonexp	∼260	∼7	∼1	∼224	∼8	∼1			
SED breakdown	130	3.5	0.5	607	17	2.1	112[f]	8	1.0
entanglement	30000	810	118	17000	607	76	3780[g]	270	34

[a] 37 g/mol = 1 bond = 0.146 nm. [b] 28 g/mol = 1 bond = 0.126 nm. [c] 14 g/mol = 1 bond = 0.130 nm. [d] All-trans conformer. [e] Reference 11. [f] From the data of Benzler and Luther, ref 39. [g] Reference 41.

Table 2. Experimental Data and Physical Properties of PDMS Samples

M (g/mol)	chain length ℓ (bonds)	τ_r (ps)	η_∞[42] (cP)	η_{nm} (cP)	ρ_m[42] (g/cm^3)
88	2		0.26		0.641
162	4	6.2	0.5	0.26	0.761
340	9	8.2	1.3	0.49	0.853
770	21	9.6	4.6	0.65	0.918
1250	34	11.7	9.4	0.89	0.935
2000	54	12.9	19	1.0	0.950
3780	102	14.3	48	1.2	0.960
5970	161	16.2	97	1.4	0.966
13650	369	28.6	340	2.8	0.970
17250	466	35.1	486	3.6	0.971
62700	1695	44.2	9740	4.6	0.974
139000	3757	50.7	97700	5.4	0.977

for light perpendicularly polarized. A weak probe pulse polarized at 45° with respect to the pump polarization passes through the sample and is normally blocked by an analyzing polarizer. When the sample becomes dichroic, the probe polarization is rotated, and the probe is partially transmitted through the analyzing polarizer. The transmission through this polarizer is a direct measure of the sample dichroism. As the time delay between the pump and probe pulses increases, the anthracene molecules rotate in random directions. The dichroism and the resulting signal intensity decay, leading to a measurement of the anthracene rotation time.

Our implementation of this method and our data analysis procedure has been described in detail before.[7,36] Briefly, the output from a mode-locked Ti:sapphire laser was frequency-doubled to produce ∼100 fs pulses at 375 nm, the peak of the absorption spectrum of anthracene in PDMS. Ninety percent of the 75 mW average power was used as a pump beam to induce transient dichroism in the sample, and the remaining 10% was used as the probe beam to measure the decay of the sample dichroism. Optical heterodyne detection of the probe beam[43] generated dichroism signals free of interference from birefringence and polarizer leakage. An example of the dichroism data is shown in Figure 3.

The resulting signal is directly proportional to the standard rotational anisotropy function[1]

$$S_{dc}(t) \propto r(t)e^{-t/\tau_{fl}} \tag{11}$$

The fluorescence lifetime, τ_{fl} = 4.8 ns, is almost 1000 times longer than the anisotropy decay times and can be ignored. We have shown previously that other contributions to the dichroism signal can also be seen under the appropriate circumstances,[36] but these are too fast or too small to affect the current measurements. The time resolution of the dichroism technique is only limited by the pulse width, which is much shorter than the rotation times, even in the lowest viscosity samples.

The dichroism experiment is sensitive to thermal effects in the sample, and it requires a high average laser power. A rapidly flowing sample is needed to avoid thermal effects and the accumulation of photodegradation products. For the lowest viscosity sample, ℓ= 4 PDMS (M = 162 g/mol; η_∞ = 0.5 cP), a flowing jet was too unstable. A 1 mm path length fused silica flow cell was used instead. A poly(tetrafluoroethylene) insert was used to narrow the flow channel and increase the flow velocity in the interaction region. The accumulation of photodegradation products on the windows was slowed by treating the cell windows with dichlorodimethylsilane. The absorption of the laser through the sample was kept low (5%), corresponding to an anthracene concentration of 300 μM, to further reduce the accumulation of photoproducts. At this concentration, the absorption spectra did not show any red-shifted component due to anthracene aggregates.

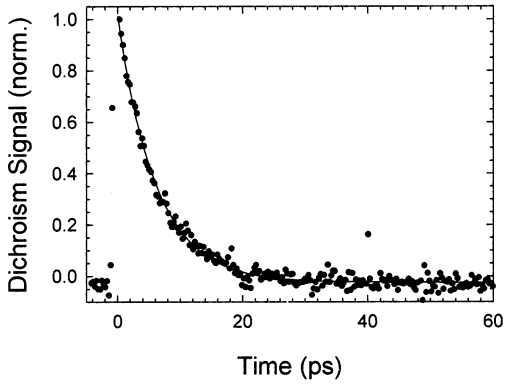

Figure 3. Dichroism decay of anthracene in ℓ= 4 (M = 162 g/mol) PDMS. The solid curve is a single-exponential fit.

Dichroism experiments with a flowing jet were used for the next six higher molecular weight PDMS samples (M = 340−5970 g/mol; η_∞ = 1.3−97 cP). In this viscosity range, the sample forms a smooth and stable jet. The path length was shorter, approximately 200 μm. Furthermore, photodegradation products do not accumulate in the jet, and so the sample concentration was increased to optimize the signal. Anthracene concentration in the jet experiments was 5 mM, corresponding to an absorption of 20%. This concentration was still low enough to prevent concentration artifacts. In all the dichroism experiments, the sample temperature was kept at 25 °C by circulating the sample through a heat exchanger immediately upstream of the flow cell or jet. The temperature of the sample was measured by a thermistor placed on the jet nozzle or in the output stream of the flow cell.

The four highest molecular weight samples (M = 13 659−139 000 g/mol; η_∞ = 340−97 700 cP) could not be measured using dichroism because the viscosities were too high to permit rapid flowing. Fluorescence depolarization measurements of these samples were made by time-correlated single-photon counting (TCSPC).[44−46] Fortunately, the rotation times in these samples were long enough to be resolved by this lower time resolution technique.

Again, our implementation of TCSPC has been described in detail before.[7] Low-intensity pulses from a different, but similar, Ti:sapphire laser were selected at an 8 MHz rate by an external acousto-optic pulse picker. After frequency-doubling, the pulses excited static samples. The sample temperature was maintained at 25 °C by thermal contact between the sample cell and an actively regulated sample block. The fluorescence polarization was selected by a 20 mm diameter Glan-laser polarizer, collected by a subtractive double monochromator, and detected by a microchannel plate photomultiplier. The emission time of fluorescence photons relative to the excitation pulse was measured by standard electronics. Time-dependent parallel $I_{\parallel}(t)$ and perpendicular $I_{\perp}(t)$ fluores-

cence decays were collected for identical lengths of time. The sample anisotropy $r(t)$ and rotation time were determined by using the relationship

$$r(t) = \frac{I_{\parallel}(t) - I_{\perp}(t)}{I_{\parallel}(t) + 2I_{\perp}(t)} \tag{12}$$

The polarization dependence of detection efficiency was reduced by placing a calcite-wedge polarization scrambler at the entrance to the monochromator. The measured ratio of parallel to perpendicular signal from an unpolarized light source was 0.96, and the parallel and perpendicular fluorescence data were weighed accordingly. The instrument response function had a full width at half-maximum of 50 ps. The anisotropy curves were fit using standard least-squares iterative convolution procedures.[44,45]

IV. Results in PDMS

Transition from Exponential to Nonexponential Decays. Paralleling the results in PIB, the rotational decay of anthracene in PDMS quickly becomes nonexponential as the polymer length increases. Only the lowest molecular weight PDMS sample has a single-exponential anisotropy decay curve (Figure 3). This sample, with a molecular formula of $Si(CH_3)_3OSi(CH_3)_3$, has a molecular weight $M = 162$ g/mol and a length $\ell = 4$. We define the length of the PDMS polymer chain in terms of the number of backbone bonds in the same way as we did for PIB (eq 3, $\sigma = 2$, $M_r = 74$ g/mol).

The transition to nonexponential decay is abrupt, and the next PDMS sample in the series, $\ell = 9$ ($M = 340$ g/mol), already exhibits the same stretched exponential shape that seen in all the longer polymers. To within the resolution of our experiments, this transition occurs at the same length in PDMS as it does in PIB.

After this transition, the decay shapes did not change any further. Independent stretched exponential fits (eq 5) to the anisotropy decays from the samples between $\ell = 9$ and $\ell = 161$ ($M = 340-5970$ g/mol) gave similar values of β for each sample. A common fit was found using the master plot in Figure 4. Each of the data sets in the master plot has been shifted along the logarithmic time axis and scaled in amplitude until the data lie on a single curve. The fact that the data do lie on a common curve indicates that they have a common decay shape.

This common shape fits well to a stretched exponential (eq 5) with $\beta = 0.68$ (cf. $\beta = 0.52$ for PIB). Using this value of β and the time shifts from the master plot, the integral average decay times for each curve were calculated using eq 6. These values are tabulated in Table 2.

The anisotropy curves of the last four samples in the PDMS series, $\ell = 369$, 466, 1695, and 3757, are not included in the master plot. Because of their high viscosity, the anisotropy decays from these samples were measured by fluorescence depolarization. The lower time resolution made measurement of the decay shape ambiguous. In the deconvolution, we assumed that the same stretched exponential shape seen in the shorter chains still applied, and good fits were obtained with this assumption. The value for the initial anisotropy for PMDS from the fluorescence depolarization experiments is 0.30, compared with $r_0 = 0.27$ in PIB and $r_0 = 0.34$ in small-molecule solvents.

Rotation Times and the Breakdown of the SED Model. The SED model predicts that the rotation time of a molecule is linearly related to the macroviscosity. Figure 5 tests this prediction by plotting rotation time

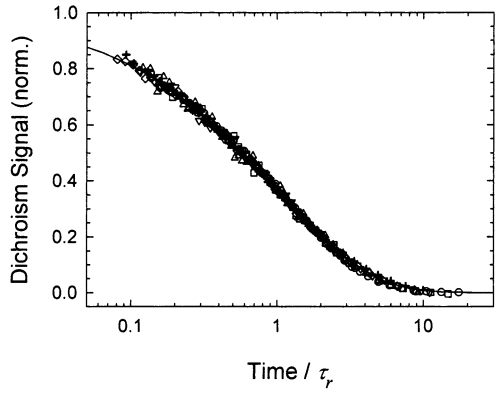

Figure 4. Master plot of the anisotropy decays in PDMS (340 g/mol ≤ M ≤ 5970 g/mol). The time scale for each data set is divided by the integral average relaxation time τ_r. The solid curve is a unit amplitude stretched exponential fit (eq 5) with $\beta = 0.68$. PDMS molecular weights: ○, 340; □, 770; △, 1250; ▽, 2000; +, 3780; ◇, 5970 g/mol.

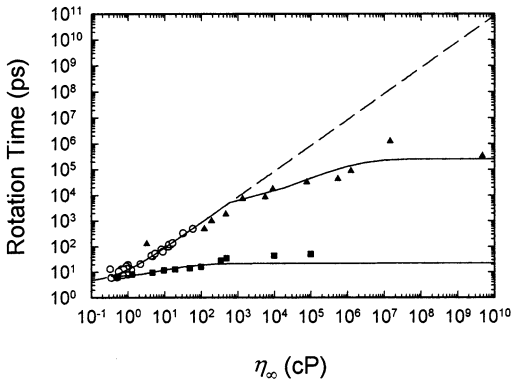

Figure 5. Rotation times of anthracene vs macroviscosity in PIB (▲) and PDMS (■) show the breakdown of the SED model. The SED model (eq 1, dashed line) is valid in small-molecule solvents (○) and short PIBs.[7] In PDMS, the rotation times diverge from the SED model for all but the shortest samples. After the SED breakdown, the rotation times slowly increase to a different limiting value in each polymer (solid curves). The solid lines are the fits of eq 8 shown in Figure 2a,c translated to the current pair of axes.

vs macroviscosity. The model works well for small-molecule solvents and for PIB's up to 2000 cP. However, only the lowest viscosity PDMS sample matches the SED prediction. In higher viscosity polymers, the anthracene rotation time is several orders of magnitude faster than the prediction based on the macroviscosity. This result is consistent with the original thesis that in a polymer the friction on a small object is reduced. Moreover, the reduction in rotational friction is several orders of magnitude different in PDMS than in PIB. This difference is qualitatively consistent with the reduced translational friction in PDMS relative to PIB indicated by the high diffusivity of small solutes (Table 3).

Two ideas about the breakdown of the SED model are eliminated by Figure 5. Many authors have modified the SED equation by changing the linear viscosity dependence to a fractional power law.[1,50] The PDMS data could be fit by such a modification. However, the PIB clearly cannot. Thus, a fractional power law is not a general way of treating the breakdown of the SED model. Previous success at using power laws can be attributed to the smaller range of solvent sizes examined and the need to include a nonzero intercept in the SED model (eq 1).[2,35,36]

Table 3. Properties and Fit Parameters for PIB, PDMS, and *n*-Alkanes

	PDMS	*n*-alkanes (PE)	PIB
T_g (K)[a]	146	150−240	200
ΔE_{ct}[b] (kcal/mol)	<0.5[c]	2.9[d]	6[e]
$\Delta E_{ct}/(k\ 300\ K)$	<0.8	4.9	10
$D \times 10^6$ (cm^2/s)[f]	1.45		3.55×10^{-4}
η^0_{nm} (cP)[g]	0.35	0.2	0.35
η^∞_{nm} (cP)[g]	2.05	8.2	3.0×10^4
A[g]	30	23	70
B[h]	0.4	0.12	0.75
l_{SED}[h]	3.5	8	17

[a] Reference 47. [b] Cis−trans barrier height. [c] References 15 and 16. [d] Reference 48. [e] Reference 14. [f] For 1,1-diphenylethane, ref 49. [g] Equation 7. [h] Equation 8.

A related idea is that the breakdown of the SED is due to "saturation" of hydrodynamics at high viscosities. However, the SED extends to very high viscosity in PIB, but in PDMS; it breaks down at viscosities much lower than where the SED model is valid for small-molecule solvents.

The failure of both of these ideas suggests that the macroviscosity is not the correct independent variable, i.e., that the rotation time is not directly derived from the macroviscosity. The inappropriate choice of axes is the cause of the complex form of the fits in Figure 5 (which are discussed below). An alternative point of view is that both the macroviscosity and the rotation time are more directly related to the polymer chain length. This approach is pursued in the next section.

Macro- and Nanoviscosity vs Polymer Length. Adopting the point of view that the rotation time reflects the viscosity on a nanometer length scale, eq 2 was used to convert the rotation times in PDMS to nanoviscosities (Table 2). This conversion allows the nanoviscosity to be compared to the macroviscosity as a function of polymer chain length (Figure 2c). In this type of plot, the region of SED behavior is reflected by identical values of the macro- and nanoviscosities, whereas the breakdown of the SED model is seen as a divergence of the macro- and nanoviscosities with increasing length. Similar measurement of nanoviscosity from rotation of a different solute [*N*-(triethoxysilylpropy)dansylamide] by Stein et al.[24] are in good agreement with our measurements (Figure 2c).

The same features seen in Figure 5 are evident in Figure 2. The macro- and nanoviscosities start at identical low values for very short PDMS but diverge for longer chains. Compared to PIB, this divergence occurs for much shorter chains in PDMS. After the divergence, the macroviscosity continues to increase substantially with chain length, whereas the nanoviscosity increases only slightly to reach the infinite chain limit. The very low friction acting on anthracene in PDMS is especially evident in Figure 2. Even for the longest, entangled polymers, the rotation time of the anthracene is as fast or faster than it would be in a 5 cP small-molecule solvent.

A fact that is more easily seen in Figure 2 is that entanglement has no effect on the nanoviscosity. The entanglement length is evident for both PIB and PDMS as a break in the macroviscosity curve (PIB $N_e = 607$, PDMS $N_e = 810$). However, no corresponding break is seen in the nanoviscosity of either PIB or PDMS.

The major difference between PIB and PDMS is the much lower nanoviscosity in PDMS relative to PIB of the same chain length. This behavior originates in the short chain region between the breakdown of the SED region in PDMS ($N_{SED} = 3.5$) and in PIB ($N_{SED} = 17$). In this region, both the nanoviscosity and the macroviscosity increase rapidly in PIB. A similar region is lacking in PDMS. The large difference in nanoviscosity is established in this region and persists to the infinite chain limit.

The PDMS data can be fit using the same empirical scheme used to fit the PIB data. Equation 7 was used fit to the nanoviscosities. This equation shows a transition between a small-molecule limit ($\eta^0_{nm} = 0.35$ cP) and an infinite chain limit ($\eta^\infty_{nm} = 2$ cP) with the transition apparently governed by the reduction in the density of end groups. The small step at the $N = 369$ PDMS point is due to a mismatch between the data collected using transient dichroism and the data collected using fluorescence depolarization. The data points from the dichroism experiments are more accurate and are favored in the fit. Because of the small range of nanoviscosities, the fit to eq 7 in PDMS is adequate, but not compelling by itself. However, the ability to use the same form that fits the PIB data is satisfying.

More significant is the ability of eq 8 to predict the macroviscosities from the fit nanoviscosities. This fit is shown in both Figures 2 and 5. (Above the entanglement length, the macroviscosities are fit to the standard $N^{3.4}$ length dependence.[51]) Equation 8 portrays the breakdown of the SED model as a transition from an SED region to a Rouse-like region. It assumes that the nanoviscosity measured by anthracene rotation is proportional to the "segmental friction" that appears in the Rouse model. The fit gives a specific measure of the characteristic length of this transition, N_{SED} (Tables 1 and 3). It also implies that once the behavior of the nanoviscosity is understood, the behavior of the macroviscosity follows from standard polymer theories.

In summary, the data show that measurements of nanoviscosity are useful in trying to understand the origin of the difference in macroscopic properties of PIB and PDMS, which occurs despite the strong analogies in structure. In fact, many of the same qualitative feature and trends are the same in both polymers. The central differences lies in the behavior of short chains and in the difference in the length where SED behavior changes to Rouse-like behavior. In the next section, we discuss a framework for understanding these differences.

V. Discussion

The experimental results presented in the previous section showed a number of phenomena that occur along the transition from small-molecule to polymeric fluid. In this section we present a possible scenario to account for all of these phenomena within a single framework. Although this scenario is not conclusively proven by the data presented above, it provides a plausible, qualitative set of hypotheses to guide future work. These ideas are very similar to the ones proposed in our previous paper,[7] but here we also discuss the differences between PIB and PDMS. In addition, we also include literature results on solute rotation in the *n*-alkanes in the comparison of different polymers.

Central to this scenario is the idea of dynamic flexibility. Measures of static structure, such as C_∞, reflect the range of conformations that a single chain can access given a long period of time. We must also ask about the range of conformations that can be accessed within a relatively short period of time. If a

polymer can access all of its potential conformations within the relevant period, it is dynamically flexible. If it cannot change conformation within the relevant period, it is dynamically inflexible. A chain that is dynamically inflexible on a given time scale may access many conformations over a longer time and thus appear flexible in measures of static structure.

Difference in the SED Breakdown Length. As noted by others, there are many similarities in the static structural properties of PDMS and PIB.[11−13] At a molecular level, the structure of PDMS results from replacing the carbon−carbon backbone of PIB with a silicon−oxygen backbone. The chain dimensions remain very similar (Figure 1). Both polymers are well above their glass transition at room temperature (Table 3). The energies of the cis and trans backbone conformers are nearly the same in each of the polymers.[9,14] As a result, measures of the static chain structure, such as C_∞ and the critical entanglement length, are very similar (Table 1). Changes in bond length and angles cause differences in the details of the chain structure[52] but not in these broad measures.

Despite these similarities in static structure, some properties of the polymers differ dramatically. For example, the diffusivity of small-molecule penetrants is much higher in PDMS than in PIB (Table 3). The macroviscosity of long-chain PDMS is substantially lower than PIB's for the same chain length. Even more dramatically, the shape of the macroviscosity vs chain length curve is different in the two polymers (Figure 2).

The differences between the two polymers show up clearly in the measurements of the nanoviscosity vs chain length. The most important difference is in the length where the macro- and nanoviscosities begin to diverge, i.e., the point of breakdown of the SED model ℓ_{SED}. In PIB, this breakdown occurs for a chain that is significantly longer than the solute, $\ell_{SED} = 17$; for PDMS, it occurs for a much shorter chain, $\ell_{SED} = 3.5$.

In our previous study of PIB, we suggested that the breakdown of the SED model is not governed by static structure but by dynamic flexibility. In this proposal, the SED model holds as long as the polymer chains remain rigid on the time scale of the solute rotation. If the chain is long enough to allow changes in torsional conformation during the rotation, a new channel for accommodating the motion of a small object opens up that is not possible for a large object. These motions are illustrated schematically in Figure 6. A rigid-chain motion (Figure 6a) involves moving the entire chain without any torsional transitions. A motion involving one torsion (an "end flip", Figure 6b) can move one end of the chain out of the way of the solute. A motion involving two torsions (a "crankshaft" motion, Figure 6c) can move a segment of the middle of the chain, without moving the two ends. Any of these motions allows movement of a small object and reduces the friction on it. However, moving a large object requires movement of the entire chain (Figure 6a). (Recall the Rouse result that the macroviscosity due a flexible chain is dominated by the longest wavelength mode.[6])

This proposal is consistent with the observed differences between PIB and PDMS. The room temperature barrier to torsional transformations in PIB is relatively high (10 kT). For short chains ($\ell < 17$), the chance of a torsional transition occurring on the chain during a rotation time is small. The macro- and nanoviscosities are both dominated by rigid-body motions of the entire chain and are the same. As the chain length increases, the chance that one of the backbone bonds will experience a torsional transition during the rotation increases. At the same time, rigid-body motion of the chains becomes increasingly difficult due to the increasing number of polymer−polymer contacts. As a result, the relevant rotational time scale increases because the viscosities are increasing rapidly with chain length. When the chain length reaches ℓ_{SED}, torsional motions within the chain become competitive with rigid-body motions for allowing rotational motion. The torsional motions do not affect the macroviscosity, so the macro- and nanoviscosities diverge.

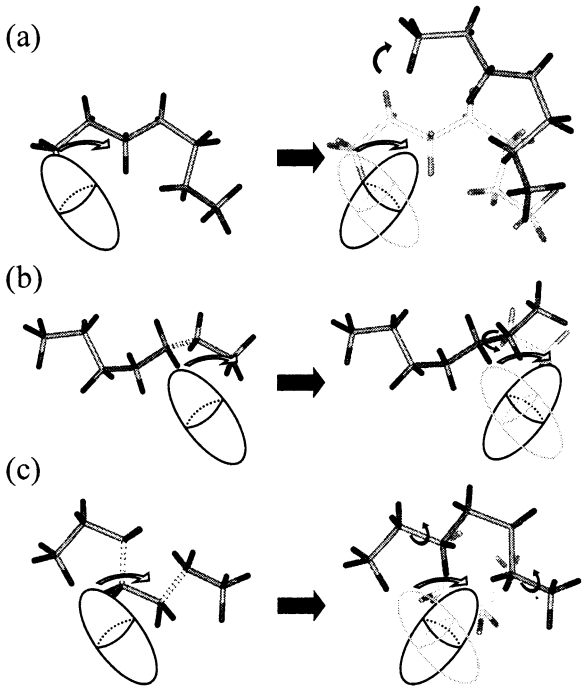

Figure 6. Schematic representation of three types of polymer motion that can accommodate rotational motion of a small ellipsoidal solute. (a) The polymer can move as a rigid body. This mechanism is most important for short polymers. It accommodates the motion of large and small objects equally well. (b) A single torsional transition (curved black arrow) can flip a section of the polymer near the chain end. (c) Two concerted torsional transitions (curved black arrows) can cause a crankshaft motion that can accommodate solute motion without moving either end of the chain. (The torsions also can be separated further.) This mechanism dominates in the long chain limit when there are few chain ends. Mechanisms b and c preferentially accommodate the motions of small objects vs large objects.

In PDMS, the torsional barriers are essentially absent (<1 kT). The torsional mechanism becomes effective for very short chains, and the macro- and nanoviscosities diverge for small values of ℓ. In the absence of rotational barriers, two other criteria affect the exact point where the SED model breaks down. First, the chain must be long enough to have torsional conformations ($\ell \geq 3$). Second, the chain must be similar in size or longer than the solute for the solute to be affected by the torsional conformations. Transforming anthracene's dimensions to the same length scales gives a range of $\ell = 3-9$, depending on the direction (Table 1). Experimentally, the SED breakdown occurs in the vicinity of the $\ell = 4$ data point, with the fit to eq 7 giving $\ell_{SED} = 3.5$. Considering the factors just discussed and the accuracy of the fit, this may represent the minimum possible value of ℓ_{SED}.

Thus, the PDMS results support the hypothesis that the breakdown of the SED model is determined by the rate of torsional barrier crossings. Other differences between PDMS and PIB can be attributed to the same mechanism. Because torsional transitions are readily accessible in PDMS, solute rotation only requires movement of short segments of the chain, even in long polymers. The nanoviscosity remains very low in the long chain limit. Given that the nanoviscosity is closely related to the segmental viscosity that underlies the macroviscosity in the Rouse regime (eq 8), the low macroviscosity of PDMS follows.

In PIB, torsional transitions are much more difficult. A region emerges where the chains are rodlike but are still dynamically inflexible ($5 < \ell < 17$). Motion is impeded by polymer−polymer contacts along the entire chain, so both the nano- and macroviscosities increase rapidly with chain length. After $\ell = 17$, solute rotation requires motion of only a segment of the chain, but a relatively long segment due to the infrequency of torsional transitions. The nanoviscosity does not increase much for longer chains, but it is already at a high level. The macroviscosity in the Rouse regime is high because of the high segmental friction that results. Overall, the presence of a distinct region where the PIB acts as a dynamically inflexible rod causes the form of the length vs macroviscosity curve to look qualitatively different in PIB than it does in PDMS.

***n*-Alkanes (PE).** A similar series of measurements in poly(ethylene) (PE) would yield an intermediate case between PIB and PDMS because the room temperature torsional barrier height in PE is intermediate (4.9 kT, Table 3). Unfortunately, PE crystallizes for chains longer than $\ell = 16$ (hexadecane), so a broad range of lengths cannot be covered easily.

Fortunately, the accessible *n*-alkanes have been studied extensively. At least 14 studies of solute rotation in the series of *n*-alkanes have been reported.[33,39,53−65] Rather than critically review all these data, we will focus on one recent and high-quality set of data by Benzler and Luther on the rotation of biphenyl in a series of 13 *n*-alkanes.[39] They found a breakdown of the SED model at the long end of this series. We will reanalyze these data from the perspective suggested by our PDMS and PIB studies.

Because the hydrodynamic volume of biphenyl has not been independently calibrated, we follow Benzler and Luther's conclusion that the SED model works for $\ell \leq 9$ (*n*-nonane) (for PE, $M_r = 14$ g/mol and $\sigma = 1$ in eq 3). In this region, the rotation time is linear in the macroviscosity, as required by the SED model. Fitting these data to eq 1 gives $\lambda V_h/6kT = 14.0$ ps/cP and $\tau_0 = 1.8$ ps for biphenyl. Biphenyl's effective hydrodynamic volume, $\lambda V_h = 0.35$ nm^3, is similar to that of anthracene, $\lambda V_h = 0.19$ nm^3. These values were used in eq 2 to calculate the nanoviscosity in the *n*-alkanes.

The results are shown in Figure 2b. The breakdown of the SED model is indeed at a length intermediate between the length in PIB and PDMS. Fits to the same model used to describe PIB and PDMS (eqs 7 and 8) work well (see Table 3). Thus, the primary role of torsional barrier crossing rates in determining this length is supported.

All previous discussions of the breakdown of the SED model in *n*-alkanes have interpreted the breakdown length as the point where the solvent size becomes comparable to the solute size. Our comparison of three different polymers makes this interpretation untenable. The breakdown of the SED model can occur for very different solvent sizes, even when the solute size is exactly the same. Our interpretation that the SED model breaks down when the solvent becomes dynamically flexible is compatible with the cross solvent comparison.

However, sensitivity to the solute size has been seen in several studies.[33,39,56,60,63] This effect is compatible with our model. The observed value of ℓ_{SED} is the length of the polymer segment that must move to allow solute rotation. If the solute is small and the solvent is dynamically inflexible, this length is determined by the average distance between torsional transitions on the solvent chain. However, if the solute becomes larger than this average distance, the length of the chain that must move is determined by the solute size itself. Eventually, this trend leads to a solute larger than the entire polymer chain experiencing the macroviscosity. Thus, we expect to see an effect due to solute size when the solute size is close to or greater than ℓ_{SED}, and we suggest that this is the effect seen in previous studies.

Similarities in the Small-Molecule to Polymer Transformation. Transport properties such as viscosity or diffusivity are qualitatively different in high polymer fluids than in small-molecule liquids. These differences develop in several stages as the polymer length increases, the breakdown of the SED model being only one of these. The other transitions identified in PIB are similar in PDMS.

Compact to Rodlike Transition. Below $\ell = 5$, the viscosity is insensitive to the polymer size in both PIB and PDMS. This result is attributed to the compact, quasi-spherical shape of the molecules in this region. Above $\ell = 8$, the viscosities of both PIB and PDMS increase more rapidly with chain length. In this region, the molecules are rodlike; i.e., they have an aspect ratio significantly greater than one. In the case of PIB, the molecules act as dynamically inflexible rods. The macro- and nanoviscosities increase rapidly as the increasing number of polymer−polymer contacts impede rigid-body motion of the polymer chains. In PDMS, the molecules act as dynamically flexible rods. The increase in nanoviscosity is weak because torsional motions allow a portion of the polymer to move without moving all the polymer−polymer contact on the chain. The macroviscosity also increases due to a Rouse-like mechanism, but not as rapidly as in the case of a dynamically rigid rod. However, the position of the compact to rod transition is the same in both PIB and PDMS.

Exponential-to-Nonexponential Transition. In both PIB and PDMS, there is a transition from exponential to stretched-exponential decays. After this transition, the shape of the relaxation remains invariant. To within our experimental resolution, the transition occurs near $\ell = 8$ in both polymers.

We attributed this transition to the development of a distribution of shapes of the polymer chains. This distribution requires both the ability to form multiple conformers and a significant change in shape, i.e., aspect ratio, among those conformers. These conditions are consistent with the observed transition length. Not surprisingly, the development of differently shaped conformers is closely linked to both the compact-to-rod transition and to the development of multiple freely jointed segments (C_∞). To within our resolution, the development of all these important characteristics of a

polymer occurs at the same length.

End Effects and Nanoviscosity. After the breakdown of the SED model, the nanoviscosity might be expected to become independent of the chain length. It is clear that, in the infinite chain limit, the nanoviscosity must reach a limiting value. However, in both PIB and PDMS, there is a small, but definite, increase in the nanoviscosity over a substantial range of intermediate chain lengths. In PIB, the fit to eq 7 made a compelling argument that this intermediate region is due to the elimination of end effects. Near ℓ_{SED}, end flips that involve only a single torsion (Figure 6b) are the most important torsional relaxation. As the chain becomes longer and end groups more infrequent, the solute rotation must be accommodated by crank shaft motions in the middle of the chain (Figure 6c). Because these motions require two simultaneous torsions, they are less common and hence less effective at reducing the viscosity. The nanoviscosity continues to rise until end flips become unimportant.

In PDMS, the fit to eq 7 is adequate, but less compelling. We believe that this is because of the smaller variation of the nanoviscosity and increased experimental error in using two different experimental techniques across this region. Relying on the analogy with PIB, it seems most likely that the small increase in nanoviscosity after ℓ_{SED} in PDMS is also due to the elimination of end flips.

Rouse Regime of Macroviscosity. Between ℓ_{SED} and the critical entanglement length, the macroviscosity in both PIB and PDMS increases significantly. In both cases, the macroviscosity can be predicted from the nanoviscosity by using a Rouse model modified to incorporate the fact that Rouse model fails below a certain length scale (eq 8).

The success of this simple formula shows that the nanoviscosity measured by our methods is closely related to the segmental friction widely discussed in connection with the Rouse model.[6] The success in fitting the macroviscosity also shows that the substantial differences in macroviscosity between PIB and PDMS of the same chain length are due to differences in the nanoviscosity. In both polymers, the same Rouse-like mechanism is responsible for generating the macroviscosity from the nanoviscosity.

Entanglement. In both PIB and PDMS, crossing the entanglement length has no significant effect on the nanoviscosity. According to our interpretation, the nanoviscosity should not be sensitive to the properties of the polymer chain further away than the first torsional relaxation, i.e., a distance of approximately ℓ_{SED}. Although this distance is different in PIB and PDMS, it is much less than the distance between entanglements in either case. Thus, the lack of an entanglement effect on the nanoviscosity is quite reasonable.

By using our measurement of the nanoviscosity and eq 8, the Rouse contribution to the viscosity can be extrapolated passed the entanglement length (Figure 2). It is interesting to speculate whether an object larger than ℓ_{SED}, but smaller than ℓ_e, would experience this viscosity.

Comparisons to Other Work. *Neutron Scattering in Pure Polymers.* Two recent studies, one experimental and one theoretical, also address the role of torsional relaxation in determining the viscosity at short length scales in polymers. In both cases, the dynamics at variable wavelengths in a pure polymer of fixed length were measured, rather than the dynamics of a small solute in polymers of variable length as was done here. If we allow for some reasonable assumptions in translating between the two approaches, a comparison of the basic conclusion of these studies can be made.

Richter and co-workers used neutron spin echoes to measured the dynamics structure factor of PIB and PDMS as a function of momentum transfer Q. They found that the Rouse model worked well in PIB for momentum transfers in the range $Q = 0.04-0.15$ Å^{-1} but found increasing discrepancies at $Q = 0.20$ Å^{-1} and below. In terms of a length, the discrepancies begin at $(Q/2\pi)^{-1} = 31$ Å. In our experiments, we found that the Rouse model connects macro- and nanoviscosity for chains with $\ell \gg \ell_{SED}$, but the Rouse model deteriorates upon approaching ℓ_{SED} and fails completely below ℓ_{SED} (eq 8). Our value for ℓ_{SED} corresponds to an all-trans chain length of 21 Å. Given the differences in the way this distance is measured, our result is in reasonable agreement with the neutron scattering study.

In PDMS, Arbe et al. found no deviations up to $Q = 0.39$ Å^{-1},[13] meaning that the breakdown length was shorter by a factor of 2 or more. In our measurements, we also found the ℓ_{SED} was much shorter in PDMS than in PIB by almost a factor of 5. Again, our results are compatible with the neutron scattering results. We attribute the shorter ℓ_{SED} to a the lower torsional barriers in PDMS. The neutron scattering group has described the breakdown of the Rouse model in terms of an internal viscosity caused by torsional barriers.[13,27−30] Although the details of the two descriptions are different, they agree on the fundamental mechanism.

Krushev, Paul, and Smith simulated the dynamic structure factor of polybutadiene to look at the effect of torsional barriers.[66] Upon artificially removing the torsional barriers in their polymer model, they found no deviation from the Rouse model up to $Q = 0.3$ Å^{-1}. They conclude that torsional barriers are not the primary cause of the breakdown of the Rouse model but suggest that collective, interchain effects are.

At this time, the reason for the discrepancy between the experimental and theoretical studies is not apparent. However, we note that the relevant barrier heights in polybutadiene are intermediate between those of PIB and PDMS. Given the factor of 5 change between the values of ℓ_{SED} in PIB and PDMS, the breakdown length in polybutadiene could be 2−4 times shorter than in PIB. Such a length would be shorter than the lengths examined in the theoretical study, but still longer than in PDMS.

Solute Transport Measurements. Implicit in the definition of a nanoviscosity are two important assumptions. First, that the nanoviscosity is a solvent property that should be transferable to a variety of different solutes in the same size range. Second, the nanoviscosity measured by rotation should be transferable to other hydrodynamic processes, such as diffusion.

Three other studies in PDMS can be used to partially test these assumptions: measurements of diffusion constants vs polymer length for two solutes by Chu and Thomas,[67,68] and measurements of rotation time of BTBP vs polymer length by Niemeyer and Bright.[26] None of these experiments were calibrated to absolute viscosities, so there is an arbitrary multiplicative factor that must be used to compare these measurements to the nanoviscosities measured by us and by Stein et al.[24]

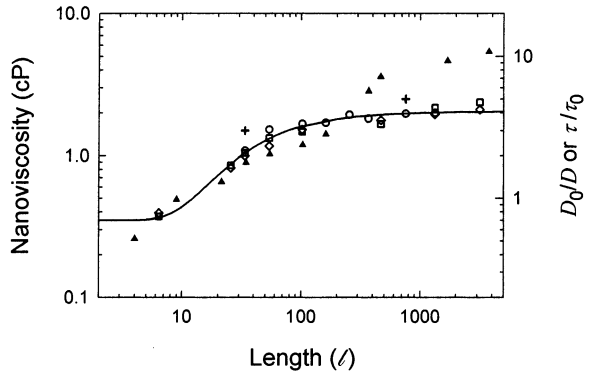

Figure 7. Comparison between our PDMS nanoviscosity data (▲) and fit (curve) and rescaled results from diffusion of pyrene in PDMS[68] (□, $D_0 = 5$ cm^2/s), phthalic anhydride in PDMS[67] (◇, $D_0 = 11$ cm^2/s), and rotation time of BTBP in PDMS[26] (○, $\tau_0 = 1.7$ ps). Nanoviscosities of Stein et al.[24] are also included (+).

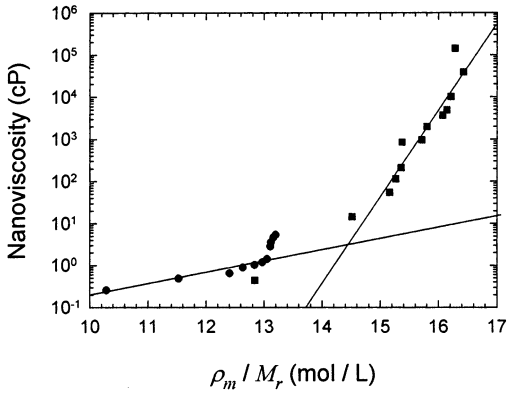

Figure 8. Nanoviscosity of PIB (■) and PDMS (●) vs density. The mass density ρ_m is corrected by the repeat unit weight M_r. Although plausible correlations with density are possible for each individual polymer (lines), it is hard to construct a density or free-volume model that will accommodate both polymers.

In Figure 7, we have chosen these factors to optimize the agreement with our fit.

All these experiments agree on the qualitative result that the nanoviscosity in PDMS is much lower than the macroviscosity. There is even reasonably good quantitative agreement, considering the variety of experimental methods used in the different studies. Thus, it appears that to a good first approximation the dynamics of small solutes in PDMS can be described by hydrodynamics with a modified viscosity. In particular, we conclude that the torsional relaxations that dominate the rate of rotation are also the most important factor in the translational diffusion of small solutes.

We should note that these prior studies have generally attributed the low nanoviscosity in PDMS to a high "free volume"[67,68] and have emphasized correlations with the density.[26] Free volume theories are seldom used to describe small-molecule liquids, for two major reasons. First, the definition of the "occupied volume" is a sensitive and hard to define parameter. Second, the probabilities of creating the large open cavities postulated in these models is extremely small. Nonetheless, free-volume models remain a popular method of correlating results in polymers.[6]

Free-volume theories are based on the static structure of the polymer and contrast strongly with our explanation in terms of torsional barriers, which is a purely dynamical property. Our comparison of two structurally similar, but dynamically different, polymers should distinguish between these explanations.

Figure 8 shows our nanoviscosities for PDMS and PIB vs density on a semilog plot. The different masses of the repeat units have been corrected for; i.e., we plot the number of repeat units per volume. For each polymer individually, a plausible, but imperfect, correlation with density can be found. By subtracting the appropriate value for the occupied volume, a correlation with the free volume could be found. However, the slopes of the two polymers are very different. It is difficult to envision a method of correcting for occupied volume that would put the data from both polymers on a single line. We believe that correlations of the nanoviscosity to the density are a fortuitous result of the correlation of each property to the chain length and not the result of a direct causative connection.

VI. Conclusions

This paper has looked at the development of the unique mesoscale properties of polymers as the chain length increases. In particular, we have measured the rotational friction on a nanometer-sized molecule to define a "nanoviscosity". Comparing new measurements in PDMS with those previously reported in PIB shows many similarities in the transition between small-molecule and polymer behavior. The development of mesoscale behavior shows several stages that appear at similar chain lengths in both polymers: a change from compact to rodlike, a change from conformational homogeneity to heterogeneity, and the loss of end-flipping contributions to the nanoviscosity. In both polymers, the entanglement threshold has no effect at the nanometer length scale.

Despite these similarities and similarities in many standard measures of static chain structure, both the macro- and nanoviscosity of PIB are several orders of magnitude higher than in PDMS in the long chain limit. This difference can be attributed to a significant difference in the transition from SED behavior to Rouse-like behavior, which occurs at short chain lengths. Because of its high torsional barriers, PIB behaves as a dynamically rigid rod until the chain length becomes quite long ($\ell_{SED} = 17$). At this length, SED behavior is lost, and Rouse-like behavior begins. PDMS, which has almost barrierless torsional motion, skips the region of rigid-rod behavior, and SED behavior is lost for very short chains ($\ell_{SED} = 3.5$). Although this difference has significant consequences for the macroscopic viscosity, it is more easily discerned in measurements at the nanometer length scale.

In the interpretation given in this paper, a central role is given to a dynamic correlation length that is defined as the length of chain over which a change in conformation is likely *within the time scale of the relevant mesoscopic process*. This measure of dynamic flexibility is quite different in PIB and PDMS, despite the similarity of the static flexibility of the two polymers. This length scale is found to be the major cause of the loss of the SED behavior characteristic of small-molecule fluids. This dynamic torsional correlation length also governs the magnitude of the nanoviscosity in the polymer and thereby the macroviscosity in the Rouse regime.

The loss of SED behavior in *n*-alkanes was reanalyzed in this context and shown to be consistent with the PIB and PDMS data. We conclude that the solute-to-solvent size ratio, which was the primary focus of previous

interpretations of the *n*-alkane data, plays a secondary role to the issue of dynamic flexibility.

Although the current measurements are limited to rotational motion, it is a reasonable hypothesis that the same mechanisms control the translational friction that governs the diffusivity of small penetrants in polymers. In small-molecule solvents, the SED model predicts that the translational diffusion constant D is linked to the rotation time through the viscosity

$$\frac{1}{3(6\lambda V_h)^{1/3}}\frac{1}{D} = \frac{\eta}{kT} = \frac{6}{\lambda V_h}\tau_r \qquad (13)$$

In polymers, this relationship may be generalized by assuming that the link between τ_r and D is through the nanoviscosity, not the macroviscosity. This hypothesis is consistent with the finding that the high diffusivity in PDMS relative to PIB is mirrored in the nanoviscosity. Existing measurements of diffusion vs chain length in PDMS are also consistent with this hypothesis.[67,68]

These observations also lead to speculation about the more general behavior of nanoparticles in polymers. How large must a particle be before it experiences the friction of a macroscopic object? Are there important length scales other than the macroscopic and nanometer scale examined here? What is the viscosity experienced by objects larger than the dynamic torsional correlation length, but below the entanglement length, or for objects smaller than the chain width? We hope that the current investigation will be a useful starting point for examining these questions.

Acknowledgment. This work was supported by the Office of Naval Research through the University Research Initiative Grant N00014-97-1-0806.

References and Notes

(1) Fleming, G. R. *Chemical Applications of Ultrafast Spectroscopy*; Oxford University Press: Oxford, 1986.
(2) Alms, G. R.; Bauer, D. R.; Brauman, J. I.; Pecora, R. *J. Chem. Phys.* **1973**, *58*, 5570.
(3) Crank, J., Park, G. S., Eds. *Diffusion in Polymers*; Academic Press: London, 1968.
(4) Vieth, W. R. *Diffusion in and Through Polymers*; Hanser Publishers: Munich, 1991.
(5) Ferry, J. D.; Landel, R. F.; Williams, M. L. *J. Appl. Phys.* **1955**, *26*, 359.
(6) Ferry, J. D. *Viscoelastic Properties of Polymers*, 3rd ed.; John Wiley & Sons: New York, 1980.
(7) Sluch, M. I.; Somoza, M. M.; Berg, M. A. *J. Phys. Chem. B* **2002**, *106*, 7385.
(8) Parameter values quoted in this paper are derived from the procedures defined here and may vary slightly from the parametrization in ref 7.
(9) Bahar, I.; Zuniga, I.; Dodge, R.; Mattice, W. L. *Macromolecules* **1991**, *24*, 2986.
(10) Vacatello, M.; Yoon, D. Y. *Macromolecules* **1992**, *25*, 2502.
(11) Fetters, L. J.; Lohse, D. J.; Richter, D.; Witten, T. A.; Zirkel, A. *Macromolecules* **1994**, *27*, 4639.
(12) Fox, T. G.; Flory, P. J. *J. Phys. Chem.* **1951**, *55*, 221.
(13) Arbe, A.; Monkenbusch, M.; Stellbrink, J.; Richter, D.; Farago, B.; Almdal, K.; Faust, R. *Macromolecules* **2001**, *34*, 1281.
(14) Boyd, R. H.; Breitling, S. M. *Macromolecules* **1972**, *5*, 1.
(15) Grigoras, S.; Lane, T. H. In *Silicon-Based Polymer Science*; Ziegler, J. M., Feardon, F. W. G., Eds.; American Chemical Society: Washington, DC, 1990; Vol. 224, p 801.
(16) Sun, H.; Rigby, D. *Spectrochim. Acta A* **1997**, *53*, 1301.
(17) Somoza, M. M.; Sluch, M. I.; Berg, M. A. In *Femtochemistry and Femtobiology: Ultrafast Dynamics in Molecular Science*; Douhal, A., Santamaria, J., Eds.; World Scientific Publishing: Singapore, 2002; pp 289−297.
(18) Ediger, M. D. *Annu. Rev. Phys. Chem.* **1991**, *42*, 225.
(19) Gisser, D. J.; Johnson, B. S.; Ediger, M. D.; von Meerwell, E. D. *Macromolecules* **1993**, *26*, 512.
(20) Johnson, B. S.; Ediger, M. D.; Yamaguchi, Y.; Matsushita, Y.; Noda, I. *Polymer* **1992**, *33*, 3916.
(21) Sillescu, H. *J. Non-Cryst. Solids* **1999**, *243*, 81.
(22) Hall, D. B.; Miller, R. D.; Torkelson, J. M. *J. Polym. Sci., Part B: Polym. Phys.* **1997**, *35*, 2795.
(23) Chapter 12, section B5 of ref 6.
(24) Stein, A. D.; Hoffmann, D. A.; Marcus, A. H.; Leezenberg, P. B.; Frank, C. W.; Fayer, M. D. *J. Phys. Chem.* **1992**, *96*, 5255.
(25) Diachun, N. A.; Marcus, A. H.; Hussey, D. M.; Fayer, M. D. *J. Am. Chem. Soc.* **1994**, *116*, 1027.
(26) Niemeyer, E. D.; Bright, F. V. *Macromolecules* **1998**, *31*, 77.
(27) Richter, D.; Arbe, A.; Colmenero, J.; Monkenbusch, M.; Farago, B.; Faust, R. *Macromolecules* **1998**, *31*, 1133.
(28) Richter, D.; Monkenbusch, M.; Allgeier, J.; Arbe, A.; Colmenero, J.; Farago, B.; Bae, Y. C.; Faust, R. *J. Chem. Phys.* **1999**, *111*, 6107.
(29) Richter, D.; Monkenbusch, M.; Pykhout-Hintzen, W.; Arbe, A.; Colmenero, J. *J. Chem. Phys.* **2000**, *113*, 11398.
(30) Harnau, L. *J. Chem. Phys.* **2000**, *113*, 11396.
(31) Kuhn, W.; Kuhn, H. *Helv. Chim. Acta* **1945**, *28*, 1533.
(32) Allegra, G.; Ganazzoli, F. *Macromolecules* **1981**, *14*, 1110.
(33) Ben-Amotz, D.; Drake, J. M. *J. Chem. Phys.* **1988**, *89*, 1019.
(34) Williams, A. M.; Jiang, Y.; Ben-Amotz, D. *Chem. Phys.* **1994**, *180*, 119.
(35) Zhang, Y.; Jiang, J.; Berg, M. A. *J. Chem. Phys.*, in press.
(36) Zhang, Y.; Sluch, M. I.; Somoza, M. M.; Berg, M. A. *J. Chem. Phys.* **2001**, *115*, 4212.
(37) Richert, R., Blumen, A., Eds. *Disorder Effects on Relaxational Processes: Glasses, Polymers, Proteins*; Springer: Berlin, 1994.
(38) Abramowitz, M., Stegun, I. A., Eds. *Handbook of Mathematical Functions*; Dover Publications: New York, 1965.
(39) Benzler, J.; Luther, K. *Chem. Phys. Lett.* **1997**, *279*, 333.
(40) Hyde, P. D.; Ediger, M. D. *J. Chem. Phys.* **1990**, *92*, 1036.
(41) Berry, G. C.; Fox, T. G. *Adv. Polym. Sci.* **1968**, *5*, 261.
(42) *Silicon, Germanium, Tin and Lead Compounds Metal Alkoxides Metal Diketonates Silicones*; Gelest: Tullytown, PA, 2000.
(43) Alvari, D. S.; Harman, R. S.; Waldeck, D. H. *J. Chem. Phys.* **1990**, *92*, 4055.
(44) Holtom, G. R. In *Time-Resolved Laser Spectroscopy in Biochemistry II*; Lakowicz, J. R., Ed.; SPIE: Bellingham, WA, 1990; Vol. 1204, pp 2−12.
(45) Birch, D. S.; Imhof, R. E. In *Topics in Fluorescence Spectroscopy;* Lakowicz, J. R., Ed.; Plenum Press: New York, 1991; Vol. 1, pp 1−95.
(46) Small, E. W. In *Topics in Fluorescence Spectroscopy;* Lakowicz, J. R., Ed.; Plenum Press: New York, 1991; Vol. 1, pp 97−182.
(47) Brandrup, J., Immergut, E. H., Eds. *Polymer Handbook*, 3rd ed.; John Wiley and Sons: New York, 1989.
(48) Smith, G. D.; Jaffe, R. L. *J. Phys. Chem.* **1996**, *100*, 18718.
(49) Wong, C.-P.; Schrag, J. L.; Ferry, J. D. *J. Polym. Sci., Part A* **1970**, *8*, 991.
(50) Zwanzig, R.; Harrison, A. K. *J. Chem. Phys.* **1985**, *83*, 5861.
(51) Doi, M.; Edwards, S. F. *The Theory of Polymer Dynamics*; Clarendon Press: Oxford, 1986.
(52) Flory, P. J. *Statistical Mechanics of Chain Molecules*; Hanser Publishers: Munich, 1989.
(53) Philips, L. A.; Webb, S. P.; Clark, J. H. *J. Chem. Phys.* **1985**, *83*, 5810.
(54) Lee, M.; Bain, A. J.; McCarthy, P. J.; Han, C. H.; Haseltine, J. N.; Smith, A. B., III; Hochstrasser, R. M. *J. Chem. Phys.* **1986**, *85*, 4341.
(55) Courtney, S. H.; Kim, S. K.; Canonica, S.; Fleming, G. R. *J. Chem. Soc., Faraday Trans. 2* **1986**, *82*, 2065.
(56) Ben-Amotz, D.; Scott, T. W. *J. Chem. Phys.* **1987**, *87*, 3739.
(57) Kim, S. K.; Fleming, G. R. *J. Phys. Chem.* **1988**, *92*, 2168.
(58) Bowman, R. M.; Eisenthal, K. B. *Chem. Phys. Lett.* **1989**, *155*, 99.
(59) Schroeder, J.; Schwarzer, D.; Troe, J. *Ber. Bunsen-Ges. Phys. Chem. Chem. Phys.* **1990**, *94*, 1249.
(60) Roy, M.; Doraiswamy, S. *J. Chem. Phys.* **1993**, *98*, 3213.
(61) Jiang, Y.; Blanchard, G. J. *J. Phys. Chem.* **1994**, *98*, 6436.
(62) Jiang, Y.; Blanchard, G. J. *J. Phys. Chem.* **1995**, *99*, 7904.
(63) De Backer, S.; Dutt, G. B.; Ameloot, M.; DeSchryver, F. C.; Müllen, K.; Holtrup, F. *J. Phys. Chem.* **1996**, *100*, 512.
(64) Pauls, S. W.; Hedstrom, J. F.; Johnson, C. K. *Chem. Phys.* **1998**, *237*, 205.
(65) Singh, M. K. *Photochem. Photobiol.* **2000**, *72*, 438.
(66) Krushev, S.; Paul, W.; Smith, G. D. *Macromolecules* **2002**, *35*, 4198.
(67) Chu, D. Y.; Thomas, J. K. *J. Phys. Chem.* **1989**, *93*, 6250.
(68) Chu, D. Y.; Thomas, J. K. *Macromolecules* **1990**, *23*, 2217.

MA021181N